

Detailed Study of the X-ray Absorption in the ISM

Javier García

(Harvard-Smithsonian CfA)

Efrain Gatuuz (IVIC, Caracas → MPA), **Claudio Mendoza** (IVIC, Caracas), **Tim Kallman** (NASA-GSFC), **Tom Gorczyca** (WMU), **Lia Corrales** (MIT)

Special thanks to **Mike Nowak, Jörn Wilms & Norbert Schulz**

The Universe in High-resolution X-ray Spectra
Chandra Workshop
Cambridge, MA
August 20th, 2015

You are Here



© 1997 Jerry Lodriguss

Motivation

- The study of the physical and chemical properties of the interstellar medium (ISM) provides important information about the formation and evolution of the galaxies.
- High-energy photons interact with the ISM via scattering (by dust and grains) and/or absorption (excitation and ionization of inner K-shell electrons, mainly). Thus, X-ray observations of the ISM provide the opportunity to study the abundances and ionization fractions for a large number of elements.
- Previous studies on ISM absorption features in X-ray binary spectra have only used functional models to fit the spectrum ([Paerels+01](#), [Schulz+02](#), [Takei+02](#), [Juett+04](#), [Liao+13](#))

Interstellar Medium Multiphase Structure

Phase	Component	Temp. (K)	Constituents
Cold	Dust	$\sim 10 - 20$	MgSiO_3, \dots
	Molecules	$\sim 10 - 20$	$\text{H}_2, \text{CO}, \dots$
	Neutral Gas	$\sim 50 - 100$	$\text{H I}, \text{O I}, \dots$
Warm	Neutral Gas	$\lesssim 10^4$	$\text{H I}, \text{O I}, \dots$
	Ionized Gas	$\sim 10^4$	$\text{H II}, \text{O II-V}, \dots$
Hot	Ionized Gas	$\sim 10^6$	$\text{O VI-VIII}, \text{Ne IX}, \dots$

X-ray absorption can provide signatures of the binding of many elements in molecules or solids; the inner-shell electronic transitions are key diagnostics since the ionization state or chemical binding shifts the line energies by a predictable amount (e.g. [deVries+Costantini+09](#), [Pinto+10](#), [Costantini+12](#)).

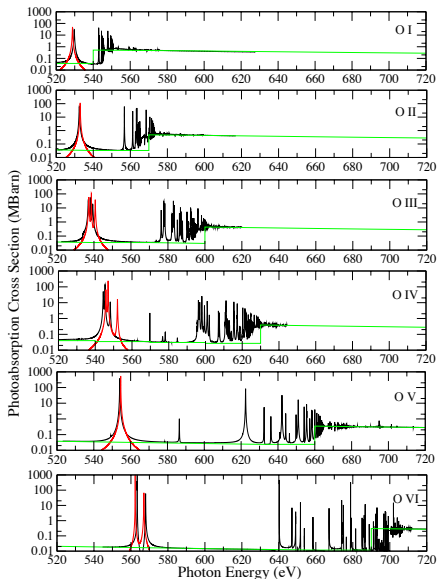
Oxygen Atomic Data

High-energy photoionization cross-sections of O ions showing the structure of the K-edge. In **black** the Breit–Pauli R-Matrix calculation by [García+05](#), in **red** those by [Pradhan+03](#), and in **green** by [Reilman+Manson79](#).

The observed flux can be approximated as

$$F(E) = F_0 \exp[-N_{\text{O}_I} \sigma_{\text{O}_I}(E)]$$

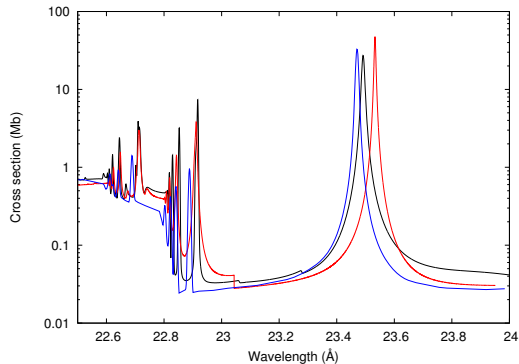
where F_0 is a normalization factor, N_{O_I} is the oxygen column density, and $\sigma_{\text{O}_I}(E)$ is the photoabsorption cross section for neutral oxygen.



(García+05)

Neutral Oxygen Atomic Data

Photoionization cross sections for neutral oxygen from [McLaughlin+Kirby98](#) (blue curve), [Gorczyca+McLaughlin00](#) (red curve), and [García+05](#) (black curve). This spectral region covers both the absorption K-edge and the $K\alpha$ absorption line (1s-2p) from O I. All the curves have been convoluted with a 0.182 eV FWHM Gaussian.



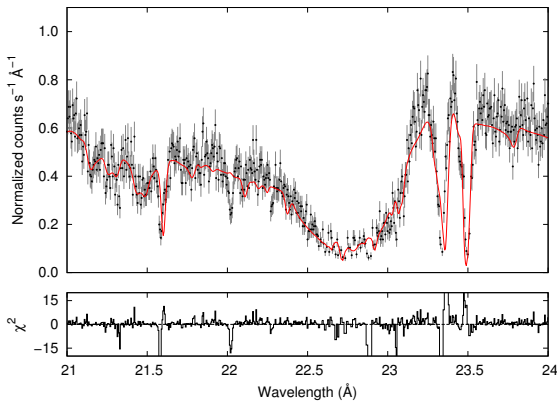
([García+11](#))

Discrepancies in the $K\alpha$ position also seen with respect to laboratory data! ([Stolte+13](#), [McLaughlin+13](#), [Bizau+15](#))

See B. McLaughlin's Poster

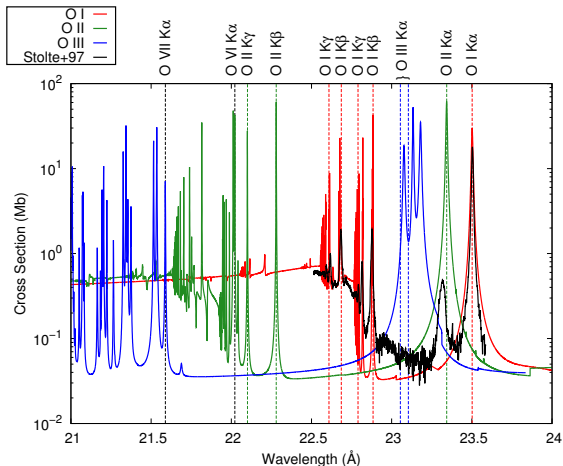
XTE J1817-330 *Chandra* Spectrum

Spectral fit of the *Chandra* MEG observations of XTE J1817-330 in the oxygen absorption region (21–25 Å) using a powerlaw*warmabs physical model.



(Gatuzz+13)

Benchmarking Atomic Data: Oxygen



O I shift: 29 mÅ

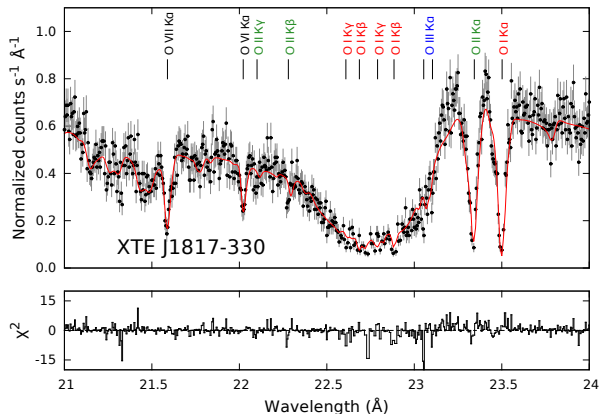
O II shift: 75 mÅ

Lab measurement also needs to be shifted!

Theoretical photoabsorption cross sections for O I (red), O II (green), and O III (blue) computed by [García+05](#) which are implemented in the warmabs model. The black solid line is the laboratory measurement by [Stolte+97](#).

(Gatuzz+13)

Benchmarking Atomic Data: Oxygen



Significant improvement
in the fit:

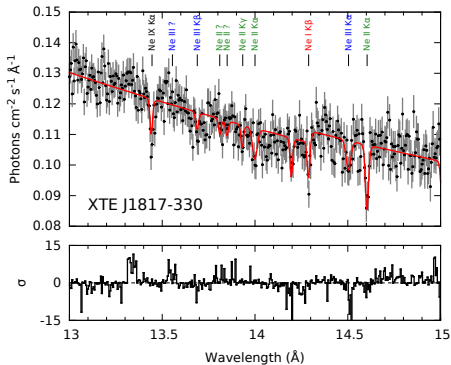
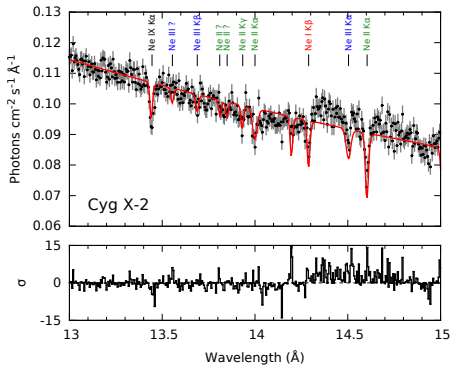
$$\chi^2 = 1.77 \rightarrow 1.25$$

O VI and O VII are fitted with Gaussian profiles (intrinsic to the source)

Spectral fit of the *Chandra* MEG observations of XTE J1817-330 in the oxygen absorption region (21–25 Å) using the **corrected** powerlaw*warmabs physical model.

(Gatuzz+13)

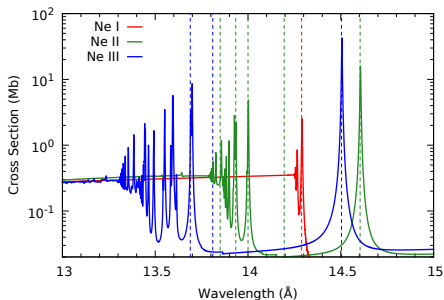
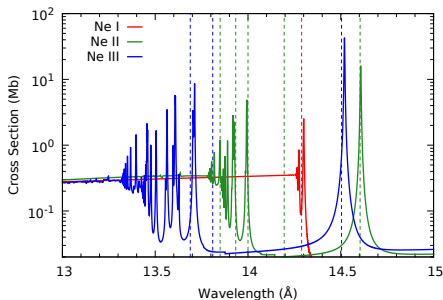
Benchmarking Atomic Data: Neon



Chandra MEG flux spectra of the X-ray binaries **Cygnus X-2** and **XTE J1817-330** simultaneously fitted with a power-law continuum and several Gaussian profiles.

Benchmarking Atomic Data: Neon

Shifts to the $K\alpha$ Resonances: Ne II = $-3.2 \text{ m}\text{\AA}$, Ne III = $-15.7 \text{ m}\text{\AA}$



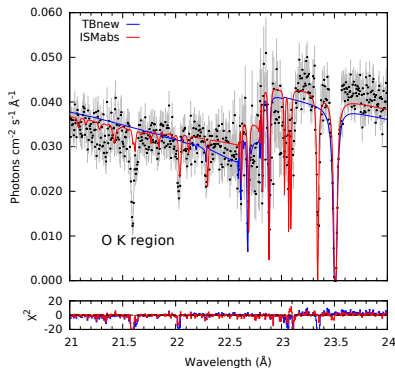
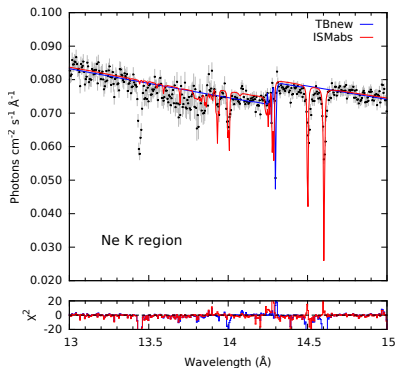
Shifts to the Cross Sections:

Ne I = $-11 \text{ m}\text{\AA}$, Ne II = $+7.6 \text{ m}\text{\AA}$, Ne III = $-14.7 \text{ m}\text{\AA}$

ISMabs: An X-ray Interstellar Absorption Model

$$I(E)_{Obs} = I(E)_{source} \exp(-\tau)$$
$$\tau = \sum_i \sigma_i(E) N_i, \text{ where } \sigma_i(E): \text{ Photoelectric Cross Section}$$

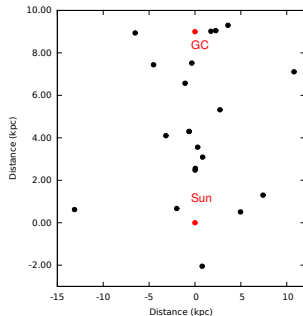
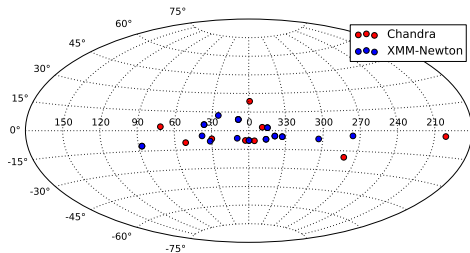
and N_i : Column Density of i -th ion.



<https://heasarc.gsfc.nasa.gov/xanadu/xspec/models/ismabs.html>

(Gatuzz, García et al. 2015)

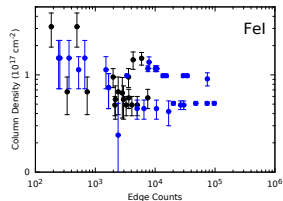
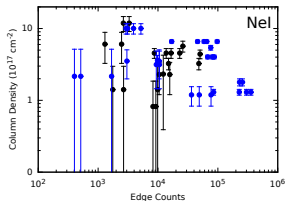
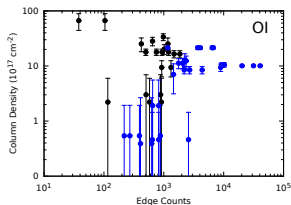
Analysis of All Available Sources



Selection of **24 bright sources**, **17** from *Chandra* and **15** from *XMM-Newton*. A total of 84 single observations were analyzed. In the case of *Chandra*, 20 observations were taken in TE-mode, and 29 in CC-mode.

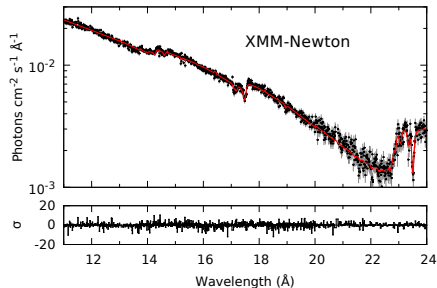
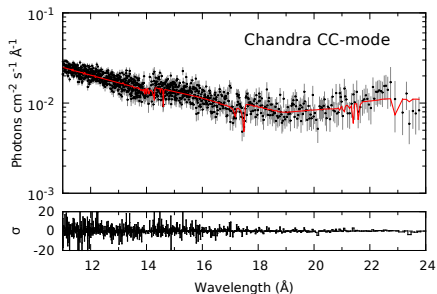
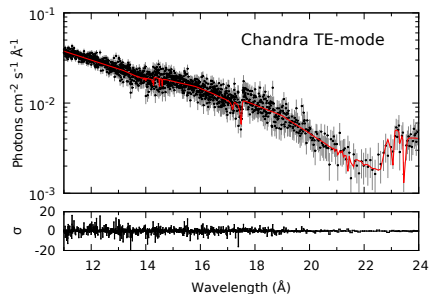
TE- and CC-Modes in Chandra

ISMabs column densities for Chandra observations versus number of counts. The **CC-mode data** shows large discrepancies when counts are low compared to the TE-mode data (**black points**).



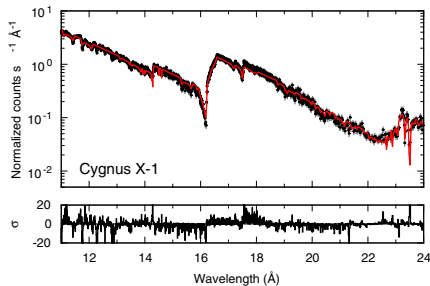
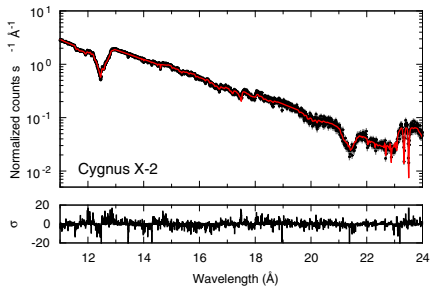
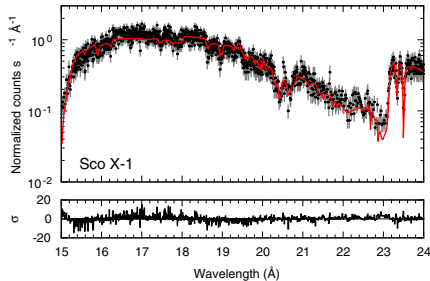
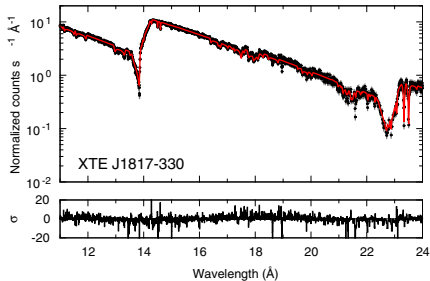
Oxygen columns from **CC-mode** data with less than 10^3 counts are **unreliable**

TE- and CC-Modes in Chandra: 4U 1636-53

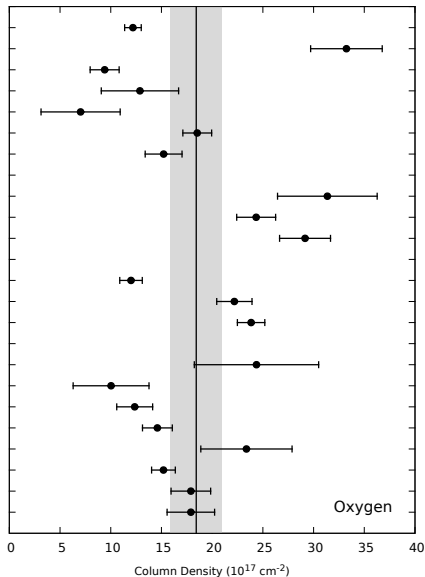
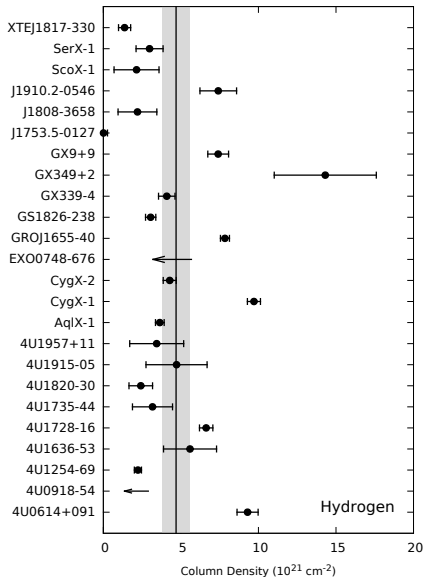


Possible **Background** contamination
at the **O-K** edge!

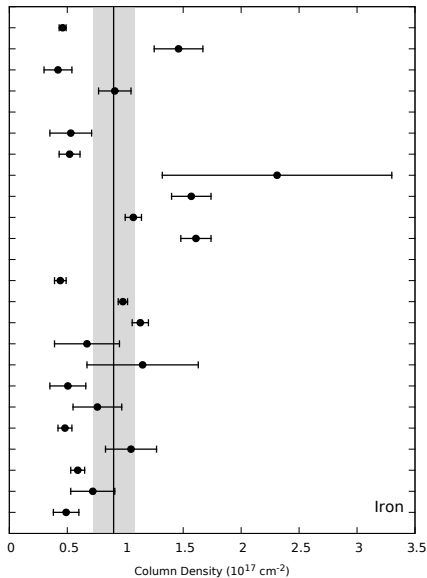
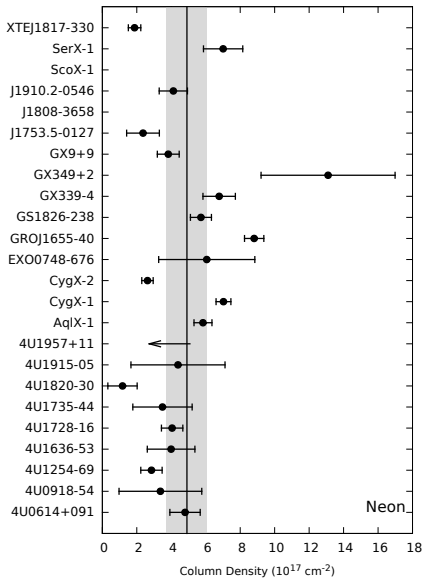
Fits to the Brightest Sources



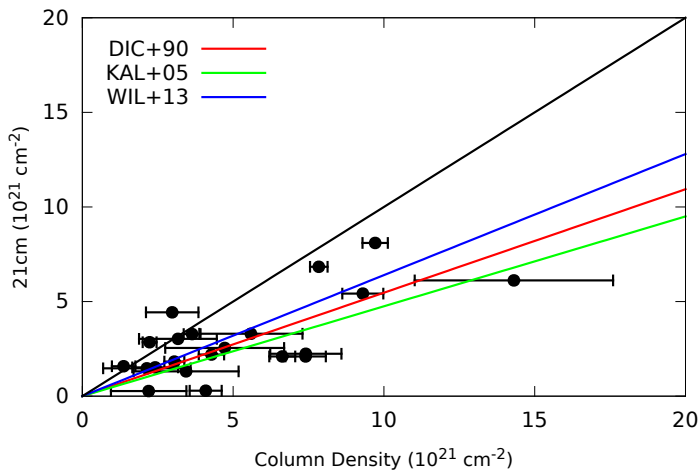
Derived Column Densities: Hydrogen and Oxygen



Derived Column Densities: Neon and Iron

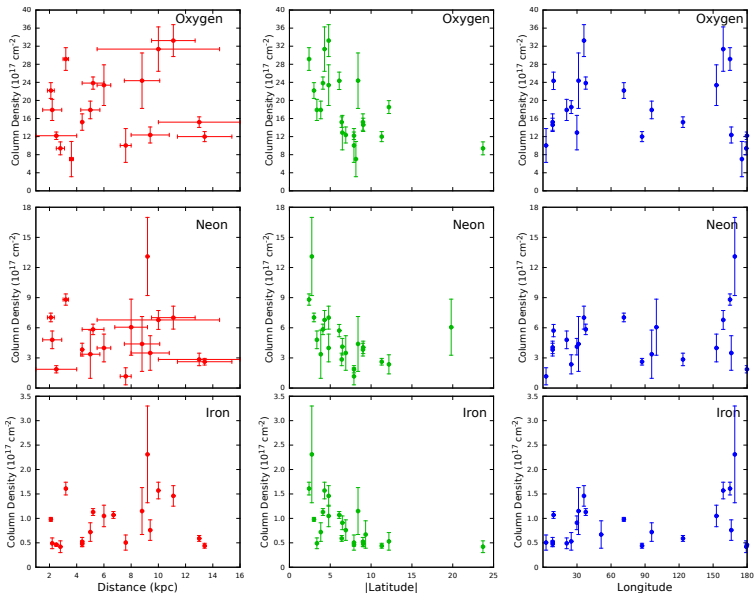


Hydrogen Column Densities

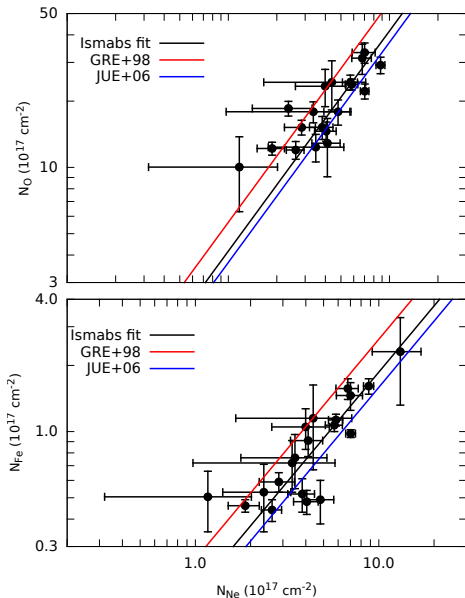


ISMabs H columns systematically larger than the 21-cm measurements by [Dickey & Lockman \(1990\)](#) and [Kalberla et al. \(2005\)](#). Better agreement with [Willingale et al. \(2013\)](#). **But continuum modeling influences this trend!**

Spatial Variations of the Columns



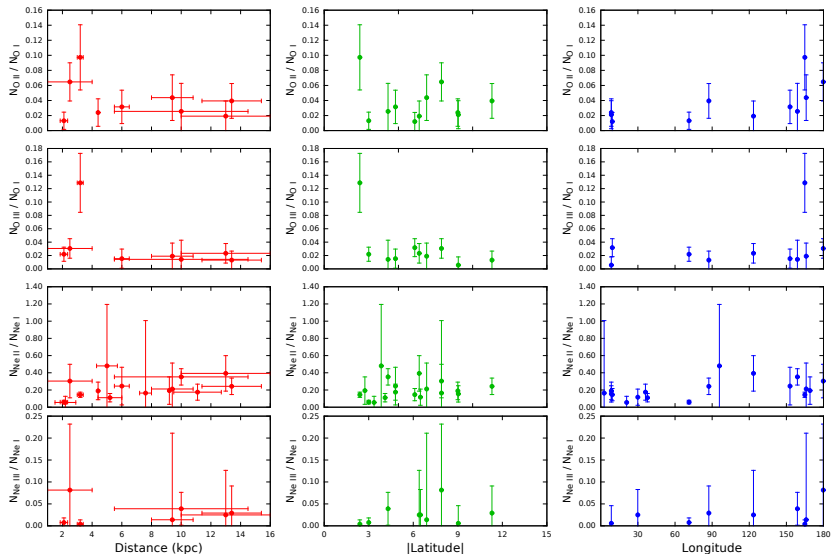
Oxygen and Iron Depletion



$$N_O = \left(\frac{A_O}{A_{Ne}} \right) N_{Ne}$$
$$N_{Fe} = \left(\frac{A_{Fe}}{A_{Ne}} \right) N_{Ne}$$

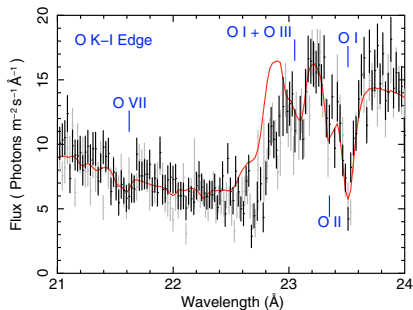
- ISMabs columns agree with those from [Juett et al. \(2006\)](#)
- Neon does not combine (noble gas)
- Depletion of oxygen and iron with respect to the Solar values of [Grevesse & Sauval \(1998\)](#)

Ion Fractions

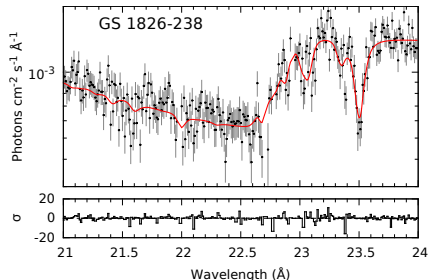


What about the Compounds?

We don't see dust or molecules, but we are not really looking for them yet.
→ But see next talk by **E. Costantini**



(Pinto+10)

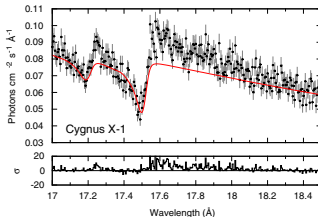
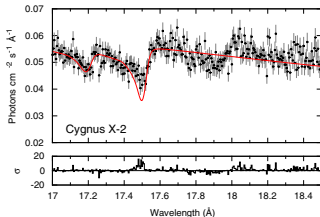
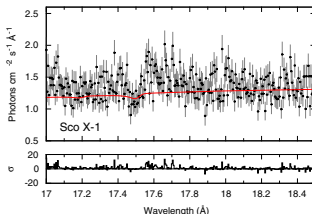
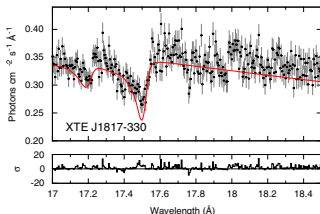


(Gatuzz+Garcia+15)

Accurate atomic data is an important step toward robust detection of **compounds**.

Fe L-shell Absorption

Only the experimental cross section for metallic Fe is included (Kortricht+Kim00)



Accurate atomic data is an important step toward robust detection of **compounds**.

Final Remarks

- The superior spectral resolution of **Chandra-HETG** allowed us to benchmark theoretical cross sections, which in turn are used for detailed studies of the ISM absorption. These models are particularly relevant for **Astro-H** and **Athena** science.
- Our analysis of **24 bright low-mass X-ray binaries** revealed absorption that includes both neutral and ionized gas, detecting for first time **$K\alpha$, $K\beta$, and $K\gamma$** resonances from some species.
- The X-ray **H column densities** are systematically larger than those from **21-cm** measurements. However, these trends can depend on the continuum model.
- Depletion of **O** and **Fe** is also detected.
- **Accurate** atomic data is the first necessary step for robust detection of **compounds**.
- A rather **large discrepancy** between several astrophysical measurements and the latest laboratory experiments still remains and needs to be solved.